Theoretical studies on the benzene molecule. II. Criticism of the ring current model

P. Lazzeretti, E. Rossi, and R. Zanasi

Citation: The Journal of Chemical Physics **77**, 3129 (1982); doi: 10.1063/1.444236
View online: http://dx.doi.org/10.1063/1.444236
View Table of Contents: http://scitation.aip.org/content/aip/journal/jcp/77/6?ver=pdfcov
Published by the AIP Publishing

Theoretical studies on the benzene molecule. II. Criticism of the ring current model

P. Lazzeretti, E. Rossi, and R. Zanasi

Istituto di Chimica Organica e Centro di Calcolo Elettronico dell'Universitá, via Campi 183, I 41100 Modena, Italy

(Received 26 October 1981; accepted 18 May 1982)

The pattern of the electron currents, induced in the benzene molecule by uniform magnetic fields, has been visualized by plotting modulus and direction of the quantum mechanical current density vector evaluated within the coupled Hartree–Fock approximation assuming a basis set of 198 CGTOs. The electron motion is characterized by axial and toroidal vortices and the paramagnetic σ circulation overcomes the diamagnetic π ring current. Intense localized circulations occur about carbon nuclei and carbon–carbon bonds, which give rise to important deshielding effects upon protons. The delocalized currents are most intense in the environment of carbons; delocalized currents are also present, and no actual "superconductivity" of π electrons can be accounted for. The reported results document that London's ring current is a rough oversimplification, affected by some unnecessary and unphysical hypotheses.

I. INTRODUCTION

According to the results presented in a previous paper,[1] the ring current model (RCM) is not completely satisfactory in order to rationalize the magnetic properties of the benzene molecule. In particular, the theoretical shielding tensor of carbon is characterized by a large negative xx component $\simeq -56$ ppm assuming a right-handed coordinate system, with the positive x axis coincident with a C–H direction and the z axis perpendicular to the molecular plane[1]: an analysis[1] of the orbital contributions to σ_{xx} reveals that roughly -70 ppm are provided by π electrons which, therefore, can be presumed to give rise to a local paramagnetic current around the C–H direction in proximity of the carbon atoms. This is confirmed by the negative value (-1.30 ppm) of the π contribution to σ_{xx} relative to the neighboring proton. Pi electrons yield a negative fraction ($\simeq -15$ ppm) also to σ_{yy} of carbon which, on the same ground, can be associated to a local paramagnetic π circulation induced by a magnetic field in the y direction. Hence, in a quantum mechanical picture, one can assume that external fields in x and y directions cause mixing of carbon $2p_\sigma$ and $2p_\pi$ orbitals which determine significant paramagnetic terms related to local anisotropy (LA) effects. The currents localized on carbon should be responsible for downfield proton shifts comparable in magnitude with those provided by delocalized electron circulations.[2,3] In fact, for benzenic protons, we estimated[1] a contribution to σ_{zz} amounting to -3.30 ppm (e.g., -1.10 to the average shielding), which would be entirely due to diamagnetic ring currents. This could seem insufficient to account for the experimental chemical shift measured in benzene PMR spectrum with respect to ethylenic systems, where the protons are similarly bonded, except that the possibility of ring currents is eliminated.[4]

In addition, the inadequacies of the RCM to rationalize the magnetic properties of cyclopropenylcation were largely evidenced in a recent paper,[5] where the fundamental role of localized circulations and the appearance of σ-paramagnetic "ring currents" were demonstrated. This pattern is worthy of careful analyses: in the present paper, we attempted to visualize the actual electron currents induced by uniform external magnetic fields through a series of plots showing modulus and direction of the quantum mechanical current density vector.[6–18] A coupled Hartree–Fock (CHF) approximation has been employed, within an LCAO approach adopting 198 CGTOs as the basis set of expansion,[1] to construct the first order perturbed wave function which appears in the current density expression.[6] The LCAO-CHF method, or coupled self-consistent field (CSCF), for approximating the quantum mechanical current is outlined in Sec. II. Section III is dedicated to the discussion of the current density maps.

II. THE CHF CURRENT DENSITY AND ITS GAUGE TRANSFORMATION

The coupled Hartree–Fock approach to the computation of induced current density has been outlined in previous papers.[19–23] In the limit of a complete set of expansion, e.g., for an exact CHF calculation, the magnetic properties, the total electron current density, and the individual MO contributions are gauge invariant.[19–24] In addition, there is a well-known connection between gauge invariance and current conservation[25] which can be recast within the usual quantum mechanical formalism.[24(b)] However, in actual CSCF calculations adopting finite basis sets, gauge invariance cannot be attained: various criteria and useful sum rules[26] were introduced to account for the degree of gauge independence of calculation, which also furnish useful indications on the degree of completeness of a basis set with respect to magnetic perturbation operators. Because of the connection mentioned above between gauge invariance and current conservation, CSCF calculations do not satisfy the continuity equation for the stationary state $\mathrm{div}\,\mathbf{J} = 0$. It seems, therefore, worthwhile to investigate the gauge dependence of CSCF current density formally. This is done here for a particular gauge transformation arising from translation of the reference coordinate system.

In a transformation of coordinates,

$$\mathbf{r} \rightarrow \mathbf{r}' = \mathbf{r} - \mathbf{d} \,, \tag{1}$$

 0021-9606/82/183129-11$02.10

the vector potential $\mathbf{A}=(1/2)\mathbf{H}\times\mathbf{r}$ undergoes a gauge transformation

$$\mathbf{A}\rightarrow\mathbf{A}'=\mathbf{A}+\nabla f(\mathbf{r}) \ , \tag{2}$$

$$f(\mathbf{r})=-(1/2)\,\mathbf{H}\times\mathbf{d}\cdot\mathbf{r} \ . \tag{3}$$

The paramagnetic Hamiltonian (in a.u.) transforms

$$\mathbf{H}^{H}=(1/2c)\,\mathbf{H}\cdot\mathbf{L}(0)\rightarrow\mathbf{H}^{H'}=(1/2c)\,\mathbf{H}\cdot\mathbf{L}(\mathbf{d}) \ , \tag{4}$$

$$\mathbf{H}^{H'}=\mathbf{H}^{H}-(1/2c)\,\mathbf{H}\times\mathbf{d}\cdot\mathbf{p} \ . \tag{5}$$

We find useful to introduce the tensor operator $h^{H\alpha}$ such as

$$\mathbf{H}^{H}=H_\alpha h^{H\alpha} \ ; \quad h^{H\alpha}=-(i/2c)\,\epsilon_{\alpha\beta\gamma}\,r_\beta\,\nabla_\gamma \ , \tag{6}$$

$$h^{H'\alpha}=h^{H\alpha}-(1/2c)\,\epsilon_{\alpha\beta\gamma}\,d_\beta p_\gamma \ . \tag{7}$$

For the diamagnetic Hamiltonian, one has

$$\begin{aligned}\mathbf{H}^{H_\alpha H_\beta}&=(1/8c^2)\,H_\alpha H_\beta[r_\gamma r_\gamma\,\delta_{\alpha\beta}-r_\alpha r_\beta]\\&=H_\alpha H_\beta\,h^{H\alpha}h^{H\beta}\rightarrow\mathbf{H}^{H_\alpha H'_\beta} \ ,\end{aligned} \tag{8}$$

$$\begin{aligned}h^{H\alpha H'_\beta}&=h^{H\alpha H_\beta}-(1/8c^2)\,[2d_\gamma r_\gamma\,\delta_{\alpha\beta}-r_\alpha d_\beta-d_\alpha r_\beta]\\&\quad+(1/8c^2)\,d_\gamma d_\gamma\,\delta_{\alpha\beta}-d_\alpha d_\beta] \ .\end{aligned} \tag{9}$$

Under transformation (2), a wave function ψ is multiplied by a phase factor

$$\psi\rightarrow\psi'=\psi\exp(-if/c) \ . \tag{10}$$

An exact Hartree–Fock molecular orbital ϕ_i is changed according to the equation

$$\phi_i\rightarrow\phi'_i=\phi_i\exp[(i/2c)\,\mathbf{H}\times\mathbf{d}\cdot\mathbf{r}]=\phi_i[1+(i/2c)\,\mathbf{H}\times\mathbf{d}\cdot\mathbf{r}+\cdots] \ . \tag{11}$$

Expanding the molecular orbitals in powers of the magnetic field

$$\phi_i=\phi_i^{(0)}+\phi_i^{(1)}+\cdots=\phi_i^{(0)}+H_\alpha\phi_i^{H\alpha}+\cdots \ , \tag{12}$$

$$\phi'_i=\phi_i^{(0)'}+\phi_i^{(1)'}+\cdots=\phi_i^{(0)}+(i/2c)\,\mathbf{H}\times\mathbf{d}\cdot\mathbf{r}\,\phi_i^{(0)}+\mathbf{H}\cdot\phi_i^{H}+\cdots \ . \tag{13}$$

Therefore, the gauge transformation for the orbitals can be written

$$\phi_i^{(0)'}=\phi_i^{(0)} \ , \tag{14}$$

$$\phi_i^{(1)'}=\phi_i^{(1)}+(i/2c)\,\mathbf{H}\times\mathbf{d}\cdot\mathbf{r}\,\phi_i^{(0)} \ , \tag{15}$$

$$\phi_i^{H'\alpha}=\phi_i^{H\alpha}+(i/2c)\,\epsilon_{\alpha\beta\gamma}\,d_\beta r_\gamma\,\phi_i^{(0)} \ . \tag{16}$$

It can be easily checked, by means of these formulas, that the current density due to the "true HF" i-molecular orbital

$$\mathbf{j}_i=(1/i)[\phi_i\nabla\phi_i^*-\phi_i^*\nabla\phi_i]-(2/c)\,\mathbf{A}\,|\phi_i|^2 \tag{17}$$

is gauge invariant, as it can be expected on physical grounds. We define [see Eq. (6)] the first-rank tensor operator

$$h^{(\mathbf{d}\times\mathbf{H})\alpha}=(1/2c)\,p_\alpha \ , \tag{18}$$

$$\mathbf{H}^{\mathbf{d}\times\mathbf{H}}=(\mathbf{d}\times\mathbf{H})_\alpha\,h^{(\mathbf{d}\times\mathbf{H})\alpha}=-(i/2c)\,\epsilon_{\alpha\beta\gamma}\,d_\beta H_\gamma\,\nabla_\alpha$$

and denote the first-order CHF orbitals corresponding to the operators $h^{H\alpha}$ and $h^{(\mathbf{d}\times\mathbf{H})\alpha}$ as $\phi_i^{H\alpha}$, $\phi_i^{(\mathbf{d}\times\mathbf{H})\alpha}$. The orbitals corresponding to the transformed operator (7) can be written [see Eq. (16)]:

$$\begin{aligned}\phi'_i&=\phi_i^{(0)}+H_\alpha\phi_i^{H\alpha}+(\mathbf{d}\times\mathbf{H})_\alpha\,\phi_i^{(\mathbf{d}\times\mathbf{H})\alpha}+O(H^2)\\&=\phi_i^{(0)}+H_\alpha\phi_i^{H\alpha}-\epsilon_{\alpha\beta\gamma}H_\alpha d_\beta\,\phi_i^{(\mathbf{d}\times\mathbf{H})\gamma}+O(H^2)\end{aligned} \tag{19}$$

so that the gauge invariance of magnetic properties is implied by the relation for HF orbitals

$$(i/2c)\,r_\gamma\,\phi_i^{(0)}=-\phi_i^{(\mathbf{d}\times\mathbf{H})\gamma} \ . \tag{20}$$

Introducing the first-order CHF functions corresponding to the operator ∇, this equation can be written

$$r_\gamma\,\phi_i^{(0)}=\phi_i^{\nabla\gamma} \ ; \quad \phi_i^{(\mathbf{d}\times\mathbf{H})\gamma}=-(i/2c)\,\phi_i^{\nabla i} \ . \tag{21}$$

In actual coupled SCF calculations, the LCAO orbitals are approximations to the corresponding HF and the deviations from Eq. (21) are a measure of the quality of the computed first-order perturbed functions. The coupled SCF first-order current density can be rewritten in terms of the CHF orbitals. In a gauge transformation, the i-orbital contribution transforms accordingly:

$$\begin{aligned}\mathbf{j}_i^{(1)'}&=\mathbf{j}_i^{(1)}+(1/c)\{[(\mathbf{H}\times\mathbf{d}\cdot\phi_i^{\nabla})\,\nabla\phi_i^{(0)}-\phi_i^{(0)}\nabla(\mathbf{H}\times\mathbf{d}\cdot\phi_i^{\nabla})]\\&\quad+\mathbf{H}\times\mathbf{d}\,|\phi_i^{(0)}|^2\} \ .\end{aligned} \tag{22}$$

By means of Eq. (21), it is easily checked that the expression within curly brackets is identically zero for HF orbitals. In coupled SCF calculations, Eq. (22) permits the evaluation of the current density for any gauge whatsoever when the results relative to a particular gauge are already at disposal. Of course, in a gauge transformation, the continuity equation is conserved for individual HF MO contributions, e.g., $\operatorname{div}\mathbf{J}^{(1)'}=\operatorname{div}\mathbf{J}^{(1)}$; the diveragence of the expression within curly brackets appearing in Eq. (22) can be rewritten as $\epsilon_{\alpha\beta\gamma}H_\alpha d_\beta V_\gamma$, where

$$V_\gamma=\frac{\partial}{\partial x_\nu}\left(\phi_i^{\nabla\gamma}\frac{\partial}{\partial x_\nu}\phi_i^{(0)}-\phi_i^{(0)}\frac{\partial}{\partial x_\nu}\phi_i^{\nabla\gamma}\right)+\frac{\partial}{\partial x_\gamma}|\phi_i^{(0)}|^2 \ . \tag{23}$$

This quantity, which is identically vanishing for HF orbitals, gives a measure of the deviation from the continuity requirements at any point in LCAO-CSCF calculations of current densities and can be used to check the quality of a basis set in different portions of the molecular space.

III. PLOTS OF CURRENT DENSITY

The CSCF current density (in a.u.) induced in benzene by a unit uniform magnetic field is visualized in Figs. 1–13, evidencing modulus and direction of the vector.[23] In every case, the gauge origin is taken on the molecular center of mass. Figure 1 shows the pattern relative to the xy molecular plane, which is a nodal plane for π electrons. As in the case of cyclopropenyl cation,[5] the most striking feature is the appearance in Fig. 1(a) of a paramagnetic interatomic loop within the molecular hexagon, which, according to a naive hydrodynamical analogy, would seem to result from the superposition of diamagnetic electron streams localized around carbon–carbon bonds. This is a strong argument against the crude RCM picture[27,28] of electron flowing, since, according to a proof of London,[28] delocalized σ currents would not be possible.[27] Within the framework of quantum hydrodynamics[7–9] and adopting the terminology of Hirschfelder *et al.*[10–15] and Riess,[16,17] the quantum mechanical streamlines form an axial vortex (AV), rotating around the center of the ring, characterized by a definite physical meaning. In particular, axial vortices have integer circulation numbers and angular momentum di-

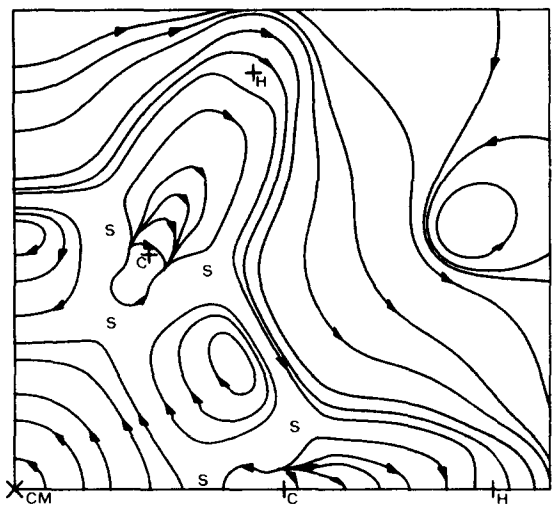

(a)

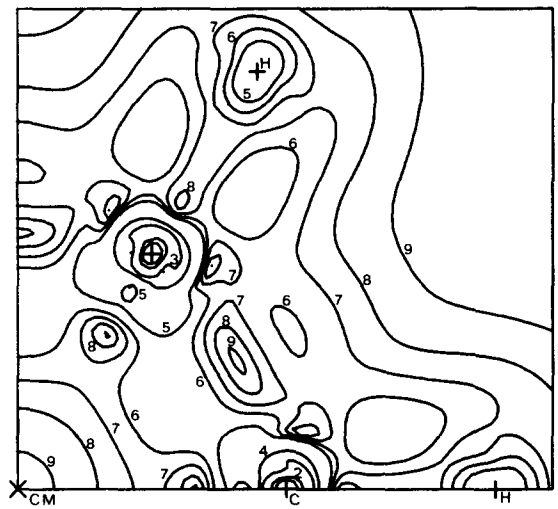

(b)

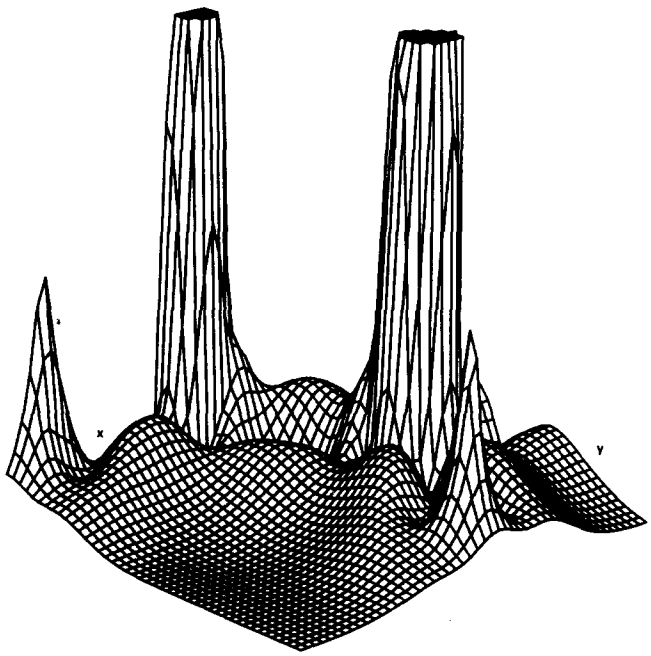

(c)

FIG. 1(a) and (b). Total electron current density in the skeletal plane. The molecule lies in the XY plane, the X direction is coincident with a C–H bond. The unit perturbing field is perpendicular to the plot, pointing outwards, e.g., diamagnetic circulations are clockwise. Stagnation points are indicated by S. The intensity can be appreciated in the contour plot of (b), where the curves are marked according to the correspondence: $1 \equiv 0.1$, $2 \equiv 0.05$, $3 \equiv 0.01$, $4 \equiv 0.005$, $5 \equiv 0.001$, $6 \equiv 0.0007$, $7 \equiv 0.0005$, and $8 \equiv 0.0003$ (all in a.u.). (c) contains a $3d$ representation of the intensity in the same molecular region, assuming the observer in front of the C–C bond. Peaks of intensity higher than 0.005 are cut.

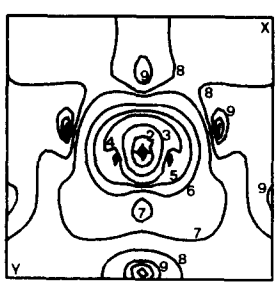

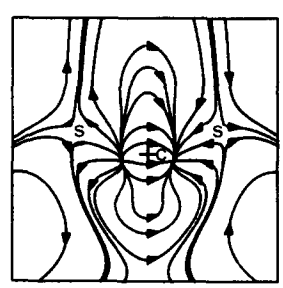

FIG. 2. Blowup of the environment of a C nucleus in the XY plane (see Fig. 1). The plots embrace a region of 2 by 2 a.u. Curves are marked according to the correspondence: $1 \equiv 0.3$, $2 \equiv 0.1$, $3 \equiv 0.03$, $4 \equiv 0.01$, $5 \equiv 0.006$, $6 \equiv 0.003$, $7 \equiv 0.001$, $8 \equiv 0.0006$, and $9 \equiv 0.0003$ (all in a.u.).

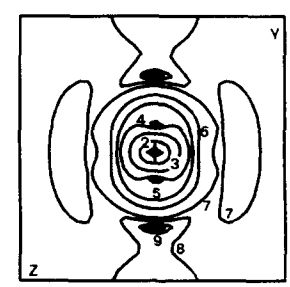

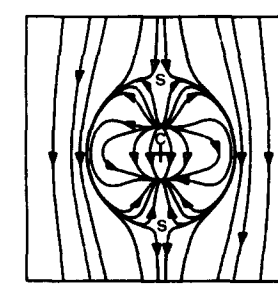

FIG. 3. Total electron density current in a plane containing a carbon and perpendicular to the plane of Fig. 2. The plots embrace a region of 2 by 2 a.u. The magnetic field is parallel to the Z axis. Curves are marked as in Fig. 2.

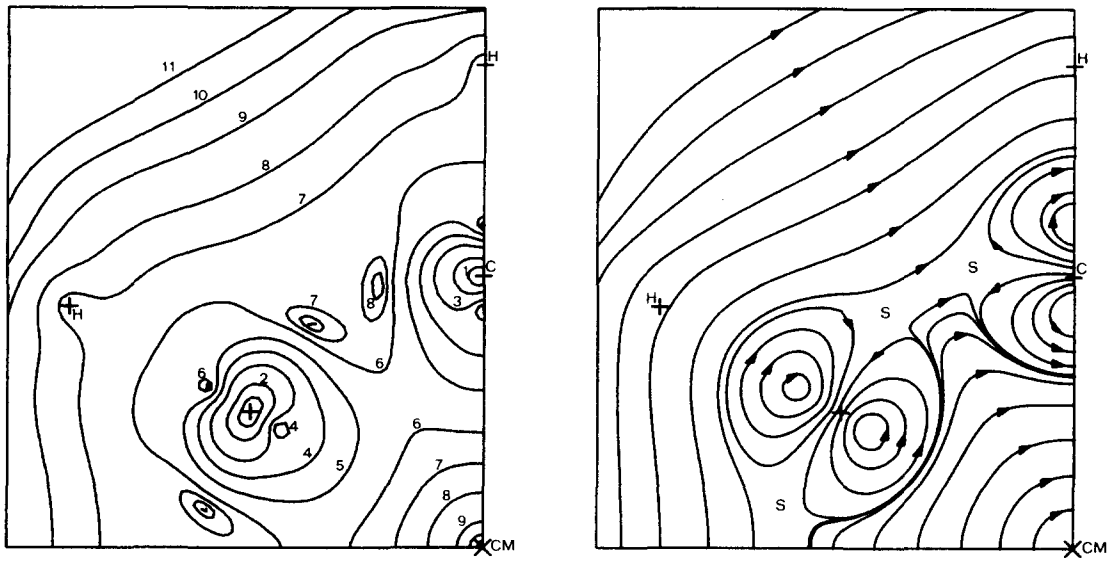

FIG. 4. Contribution to the total current density of Fig. 1 arising from $2a_{1g}$ orbital. Curves are marked according to the correspondence: $1 \equiv 5\times10^{-3}$, $2 \equiv 2.5\times10^{-3}$, $3 \equiv 1\times10^{-3}$, $4 \equiv 5\times10^{-4}$, $5 \equiv 2.5\times10^{-4}$, $6 \equiv 1\times10^{-4}$, $7 \equiv 5\times10^{-5}$, $8 \equiv 2.5\times10^{-5}$, $9 \equiv 1\times10^{-5}$, $10 = 5\times10^{-6}$, $11 = 2.5\times10^{-6}$ (all in a.u.).

pole moments (which are not quantized in the present case, since $\langle L_z \rangle$ is proportional to the field strength).[14] Such vortices flow around nodal lines determined by the intersection of a nodal surface of the unperturbed (real) wave function with a nodal surface of the perturbed (pure imaginary) wave function.[10–16] In order to understand the presence of the nodal axis passing through the center of the benzene ring, it is necessary to investigate the streamline pattern as a mixture of separate components. Within the hydrodynamical representation,[7–9] the many-component fluid is compressible, viscous, and rotational,[10–15] different components have different velocities, so that there is diffusion and one can try to analyze the role of the different molecular orbitals[14] contributing to the total stream in order to explain vortex generation. From purely topological considerations, it is readily obtained [Ref. 1(b)] that several planar aromatics are endowed with an AV flowing around the molecular center of mass, say $C_3H_3^+$, $C_5H_5^-$, C_6H_6, $C_7H_7^+$, and $C_8H_8^{2+}$. In many cases, the unperturbed and perturbed MOs, responsible for vortex formation owing to intersection of nodal surfaces, can be determined *a priori* by simple inspection of their symmetry properties [Ref. 1(b)]. In Fig. 14, relative to the skeletal plane, we evidenced the intersection between the nodal surfaces of the zero- and first-order molecular orbitals. These plots show that the central axial vortex is due to e_{1u}, e_{2g}, b_{1u}, and b_{2u} unperturbed orbitals, whose nodal surfaces cross those of the corresponding perturbed components, thus determining a

FIG. 5. Contribution of σ electrons to the current density at 0.75 bohr above the molecular plane of Fig. 1. Curves are marked according to the correspondence: $1 \equiv 0.001$, $2 \equiv 0.0007$, $3 \equiv 5\times10^{-4}$, $4 \equiv 3\times10^{-4}$, $4 \equiv 1\times10^{-4}$, $6 \equiv 5\times10^{-5}$, $7 \equiv 1\times10^{-5}$ (all in a.u.).

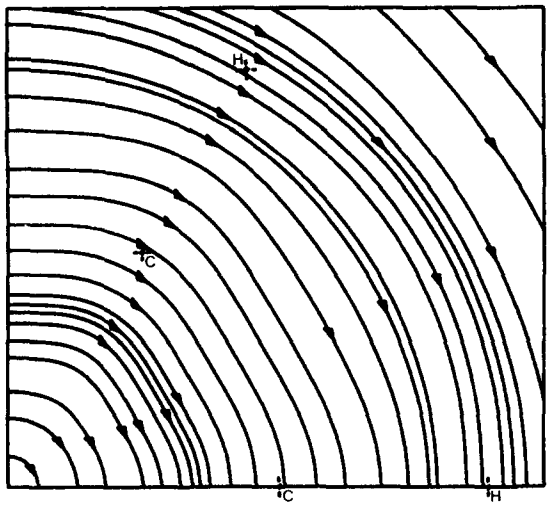

(a)

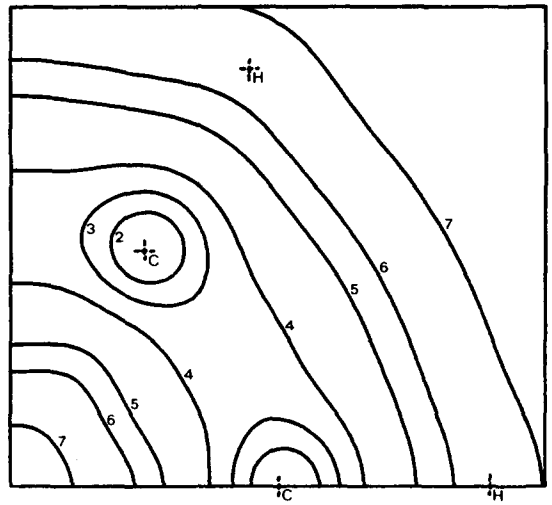

(b)

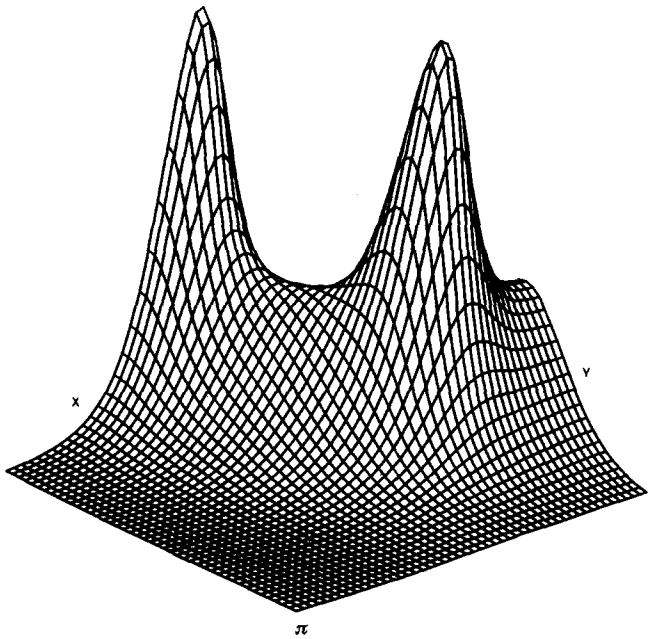

(c)

FIG. 6(a) and (b). Contribution of π electrons to the current density in the same plane as Fig. 5. Curves are similarly marked. (c) The 3*d* view of the intensity is shown according to the same observing conventions of Fig. 1(c).

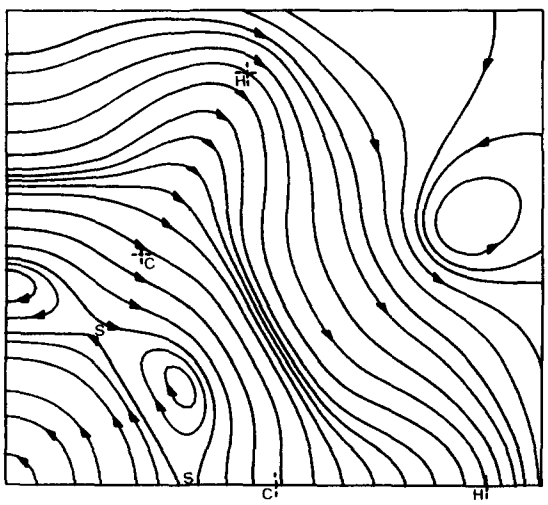

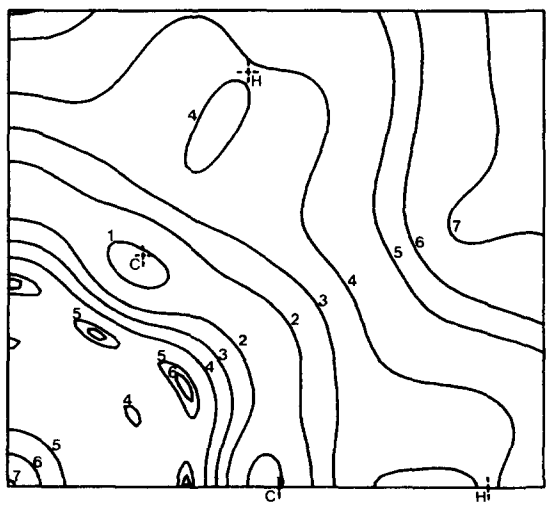

FIG. 7. Total electron current density in the plane of Figs. 5 and 6. Curves are similarly marked.

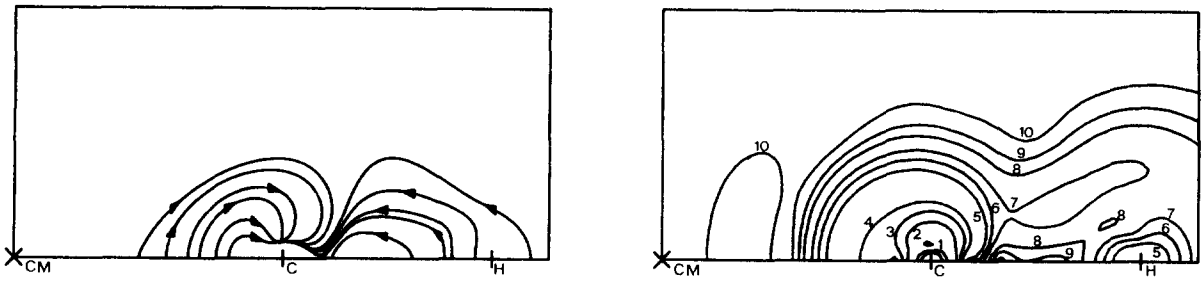

FIG. 8. Contribution of σ electrons to the current density in the XZ plane of the reference frame. The magnetic field is pointing inwards, e.g., diamagnetic circulations are counterclockwise. Curves are marked according to the correspondence: $1 \equiv 0.05$, $2 \equiv 0.01$, $3 \equiv 0.005$, $4 \equiv 0.003$, $5 \equiv 0.001$, $6 \equiv 7 \times 10^{-4}$, $7 \equiv 5 \times 10^{-4}$, $8 \equiv 3 \times 10^{-4}$, $9 \equiv 2 \times 10^{-4}$, $10 \equiv 1 \times 10^{-4}$ (all in a.u.).

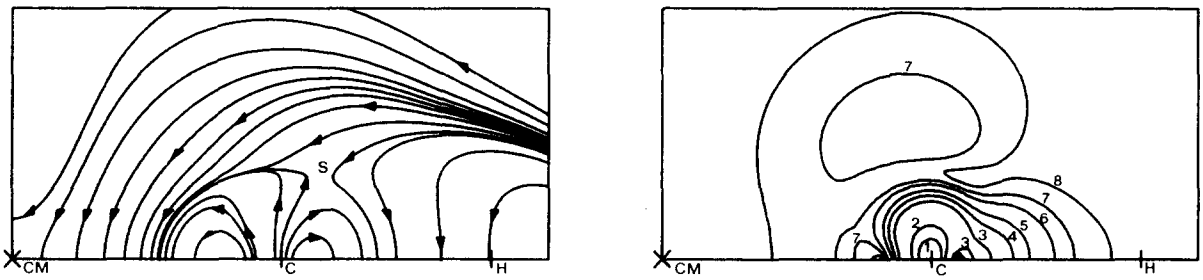

FIG. 9. Contribution of π electrons in the same plane as Fig. 8. Curves are marked according to the correspondence: $1 \equiv 0.005$, $2 \equiv 0.003$, $3 \equiv 0.001$, $4 \equiv 7 \times 10^{-4}$, $5 = 5 \times 10^{-4}$, $6 = 3 \times 10^{-4}$, $7 = 2 \times 10^{-4}$, $8 = 1 \times 10^{-4}$ (all in a.u.).

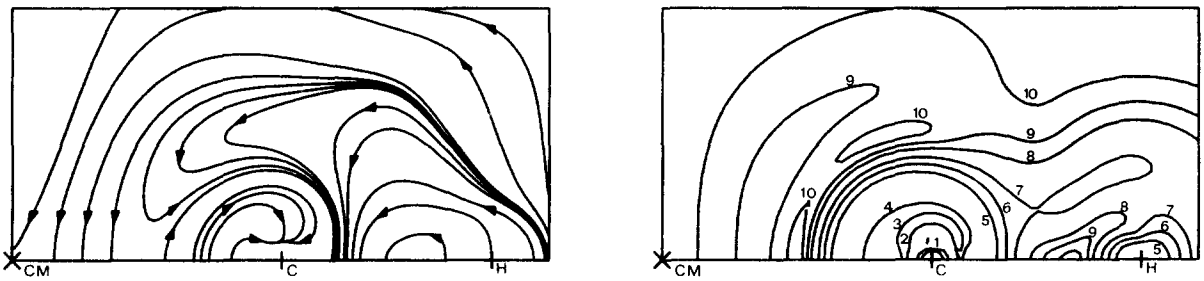

FIG. 10. Total electron current density in the same plane as Figs. 8 and 9. Curves are marked as in Fig. 8.

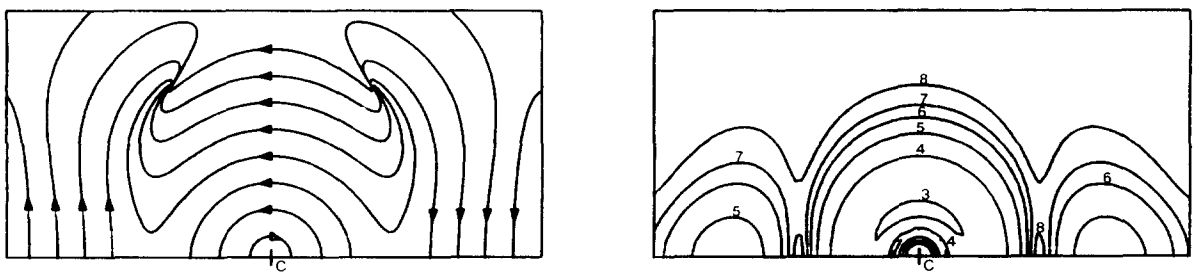

FIG. 11. Contribution provided by σ electrons to the current density in a plane containing the C atom and parallel to the YZ plane of the reference frame. The magnetic field points outwards, e.g., diamagnetic circulations are clockwise. Curves are marked according to the correspondence: $1 \equiv 0.007$, $2 \equiv 0.005$, $3 \equiv 0.003$, $4 \equiv 0.001$, $5 \equiv 5 \times 10^{-4}$, $6 \equiv 3 \times 10^{-4}$, $7 \equiv 2 \times 10^{-4}$, $8 \equiv 1 \times 10^{-4}$ (all in a.u.).

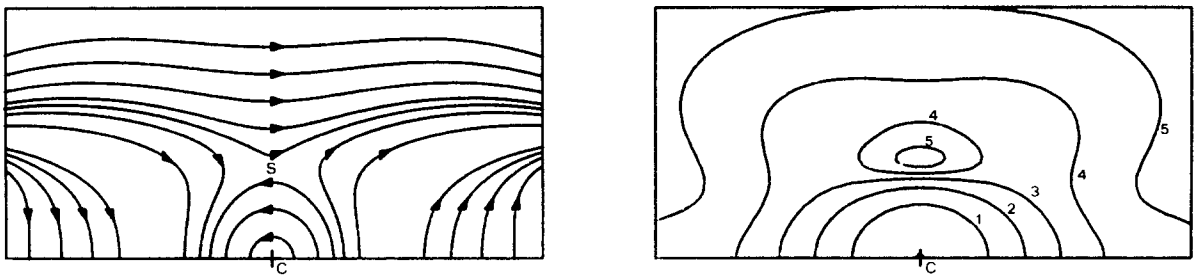

FIG. 12. Contribution of π electrons to the current density in the same plane as Fig. 11. Curves are marked according to the correspondence: $1 \equiv 0.001$, $2 \equiv 5\times10^{-4}$, $3 \equiv 3\times10^{-4}$, $4 \equiv 2\times10^{-4}$, $5 \equiv 1\times10^{-4}$ (all in a.u.).

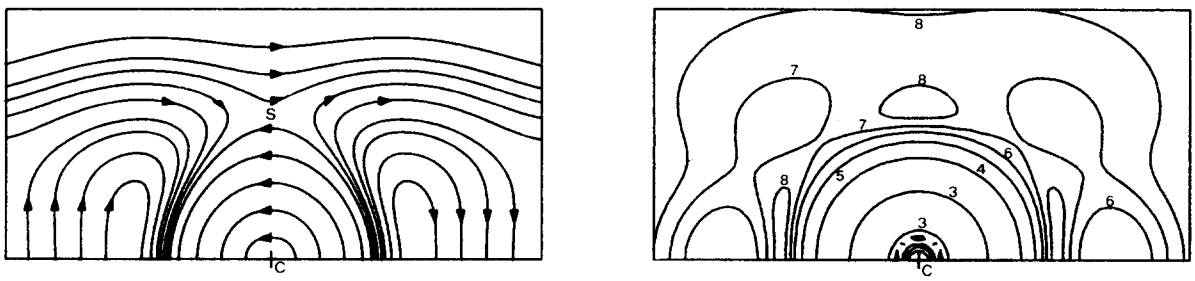

FIG. 13. Total electron current density in the same plane as Figs. 11 and 12. Curves are marked as Fig. 11.

nodal axis (z axis) coincident with C_6—the central vortex flows around this direction. In Fig. 1, delocalized σ currents flow also in the peripheral regions, which can be expected for any symmetrical system (even a hydrogen atom, as has been emphasized[27]). On the other hand a localized closed loop appears out of the ring, facing a C–C bond, in a region where there is an inlet in the charge distribution, due to the geometric arrangement of the H–C–C–H fragment. In Fig. 1(a), one recognizes the characteristic aspect of some stagnation (S) points which are the loci where J goes to zero. One of these points can be detected on the binary axis coincident with the C–H direction, in the boundary region among two localized C–C circulations and the

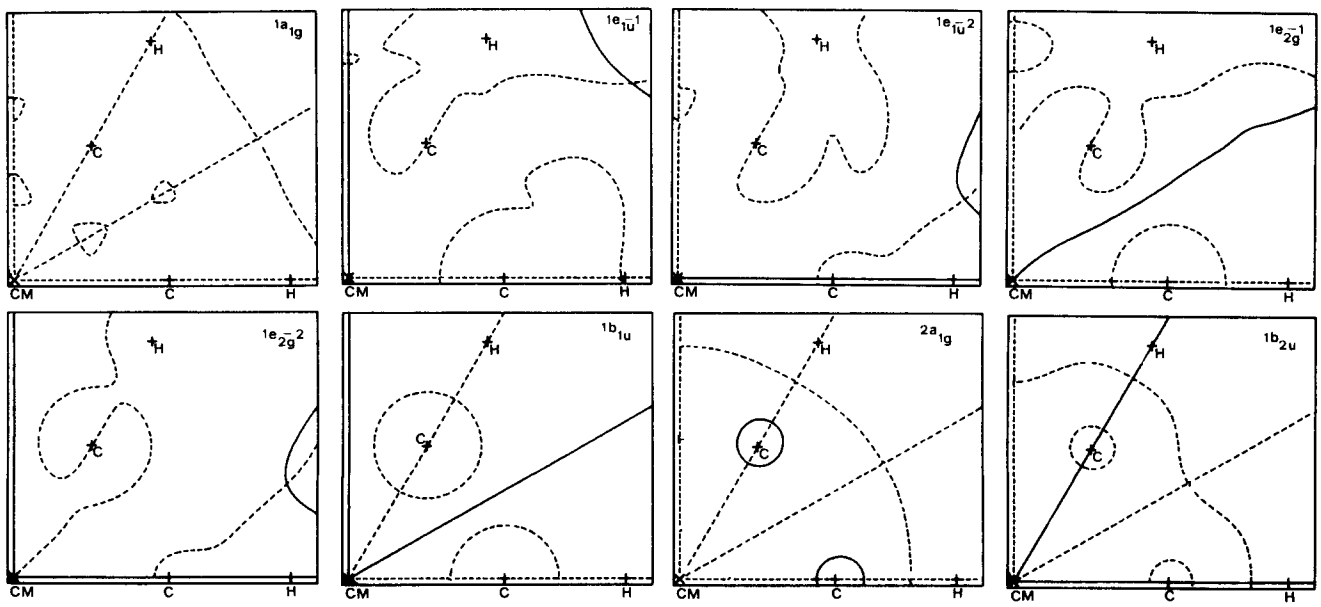

FIG. 14. Intersection between nodal surfaces of real (solid line) and imaginary (dotted line) parts of some significant molecular orbitals. Plots are relative to the molecular plane, assuming a perpendicular magnetic field.

central axial vortex. Another S point lies behind the external vortex (out of the figure) and a couple of S points are placed near a C atom, symmetrically with respect to the C–H direction. Localized circulations are found around carbon atoms, where the CHF streamlines present a rather complicate pattern.

This region of molecular space is characterized by a high node density (see Fig. 14). There are nodal lines forming close loops which are approximately circular or ovoidal, due to $2a_{1g}$, $1b_{2u}$, $2e_{2g}$, and $2e_{1u}$ orbitals. The streamlines flow up from the center and down to the sides of the nodal loop, giving rise to a quasitoroidal vortex (TV)[10–14] in this area. One must note that the torus is perpendicular to the molecular plane (see also Figs. 2 and 3). As an example of component analysis, we have shown the contribution provided by the $2a_{1g}$ orbital in Fig. 4. The general features of current flowing are easily understood by inspection of Fig. 14. The toroidal circulation is established about the loop determined by the real nodal surface (approximately a quadric) crossing an imaginary plane perpendicular to the skeletal one. In Fig. 1, two singular points are found in close proximity of each carbon, symmetrically placed with respect to the C–H direction, where there is seemingly "creation" and "annihilation" of current.

We also performed other calculations based on refined plotting grids in order to blow up the diagrams in the environment of the carbon atom. Also the corresponding maps show the presence of a source and a sink (see Figs. 2 and 3). These are essentially due to violations of the continuity equation referred to in Sec. II. In fact, another map, obtained after origin translation (not shown here) exhibits neither source nor sink near carbon, even if the general pattern deteriorates. Some close loops become spirals and other source-hole couples appear in different points. However, other features of the map are not changed in any major way when the origin is changed. We recall that the CSCF wave function[1] employed in the present study, owing to its high quality, possesses a good gauge behavior, as can be appreciated by means of AMM sum rules.[26] However, these relations, furnish useful "in the mean" indications, e.g., the actual deviations of the first-order CSCF orbitals from Eq. (21) can be still dramatically large for many r values. For the sake of simplicity, the origin of source-sink couples has also been investigated for a neon atom[29] by performing a series of minimal basis calculations with different choices of the gauge. The singularities are not found when the origin is close to the nucleus and become more and more evident when the distance between these points is increased. One possible way of circumventing this nuisance might be that of enriching the basis set of carbon in order to improve the description of charge distribution near the singularities and to fulfill Eq. (21) more satisfactorily. To this end, floating functions centered in proximity of the critical points would probably be effective. However, this task is not easy to perform in general and could be even more unpractical in the case of benzene. Improving the quality of the basis set which is already rich of 198 CGTOs would be hard to accomplish nowadays, owing to the present stage of computer development. Therefore, this matter deserves future careful analysis, which go beyond the aims of this work.

The intensity of the currents flowing in the molecular plane is displayed in Figs. 1(b) and 1(c). The most intense circulations occur around the atoms, carbon in particular, but the currents localized around the C–C bonds are also characterized by appreciable intensity. This pattern lends support to the well-known additive schemes for evaluating the magnetic susceptibilities in terms of atomic (or bond) Pascal constants. The paramagnetic stream around the molecular center has a significant weight, especially in the boundary regions near the sides of the hexagon and the intensity of the external axial vortices in the outer reaches of molecular plane is small relative to other circulations (less than 1×10^{-4} a.u., which is the smallest reported in the diagram).

The intense toroidal vortices close to each carbon atom extend up to the neighboring proton and the current density is diamagnetic in the intermediate region with higher intensity close to carbon.

As regards carbon itself, if the electronic circulation took place according to the shape of a perfect geometrical torus, the nucleus would be neither shielded nor deshielded in the z direction:

The actual pattern is that of a distorted torus, so that the local diamagnetic circulations predominate in intensity, causing a net shielding. In fact, the theoretical σ_{zz} of carbon is 190 ppm [Fig. 1(a)], compared with an experimental value of 186± 10.

Figure 5–7 examine the situation in a plane parallel to the molecular hexagon, 0.75 a.u. higher. The distance 0.75 was chosen in a first attempt to investigate the part played by π electrons, whose distribution is fairly maximum at roughly 0.5 a.u. above the carbons and 1 a.u. above the C–C bond.

Figure 5(a), which outlines the trend of the σ currents, is qualitatively similar to Fig. 1(a). In particular, paramagnetic ring currents (AV) ar found flowing around the center of the molecule, localized circulations occur around C–C bonds, the external AV in front of C–C bonds is still present, and the delocalized σ ring currents take place. This figure does not contain any unpleasant discontinuity. A comparison with the corresponding sketch relative to the skeletal plane suggests that, also there, the actual behavior in the environment of carbon might be similar to that of Fig. 5(a).

The stagnation point lying between two continuous diamagnetic loops localized around the sides of the hexagon is also evident. A couple of stagnation points appear, symmetrically placed with respect to a C–H bond, close to the axis of the toroidal circulation.

The π currents in the plane at 0.75 bohr are displayed in Figs. 6(a)–6(c). These are actually ring currents in the acceptation of London[16] and, as such, give some sense to RCM. It is interesting to observe that, even if they are sustained by only six π electrons, their intensity is comparable with that provided by 36 σ electrons in several regions of the molecular plane. An

argument in contrast with the crude RCM hypothesis of freely flowing π electrons is offered by the trend of intensities along an interatomic loop. These reach their maximum in proximity of carbon atoms and are sensibly lower (roughly 50% and more) over a C–C bond. In addition, the broad π stream of intensity 3×10^{-4} a.u., between two 4 lines, flows in a path situated approximately over the perimeter of the hexagon. Out of this loop, there is a significant decay of intensity going towards the center of the ring. The π circulation is smoothly lowering also in the tail regions, but remains diamagnetic over the proton where it is roughly ten times (or more) less intense than over the skeletal C ring.

The intensity $j=j(x,y)$ of the π current density is also visualized in Fig. 6(c) which, even more explicitly than Fig. 6(b), indicates the reinforcement about carbon nuclei. On the basis of these results, one might reasonably argue that the deshielding effects due to π electrons on the neighboring proton are, to a large extent, of local nature even if a delocalized π stream takes place since the intensity of the current density is significantly higher in the environment of carbon nuclei. In other words, the present findings would seem to assign a certain degree of reliability to the "antimodel" of Musher[27] and to his Pascalian scheme for magnetic susceptibilities based on local atomic (or bond) contributions.

According to our theoretical treatment, the π electrons cause a small reinforcement of the external magnetic field H at the proton, which is explained by RCM in terms of induced magnetic dipole parallel to H itself.[4] Our results are in partial agreement with this model, in that they support the hypothesis of a nearby π ring current. However, the total field induced by σ and π electrons has the opposite direction as the external one. In addition, the diamagnetic σ loops localized about C–C bonds are characterized by an intensity which is almost equal to that of the π stream. By replacing the currents by point magnetic dipole a la Pople,[21] one can conclude that these loops are responsible for lowering σ_{zz} of proton to a significant extent. The total current density in the plane at 0.75 bohr is shown in Fig. 7(a), which is easily understood as a result of the superposition of Figs. 5(a) and 6(a). Accordingly, this figure sketches the delocalized currents which are of σ and π nature.

The plots relative to the xz plane, which perpendicularly bisects the hexagon along an H–C–C–H direction, are presented in Figs. 8–10. (The perturbing magnetic field is assumed perpendicular to the plane of the plot, pointing inwards, e.g., diamagnetic circulations are counterclockwise.) Because of the lack of gauge invariance affecting our calculation, the direction diagrams for the σ contribution and the total current density, Figs. 8(a) and 10(a), contain a sink in proximity of the carbon atom [the situation is similar to that encountered in the molecular plane, see Figs. 1(a), 2(a), and 3(a)] which makes more difficult the interpretation of the magnetic shielding tensors of carbon and, in part, of hydrogen.

For the latter, however, inspection of diagrams reveals the existence of a low intensity diamagnetic circulation in the region of the proton, which probably provides a smaller contribution to the value of total σ_{yy}[1] than the intense nearby paramagnetic flow of π electrons, cf. the value contributed by π electrons to σ_{yy} 12.13 ppm compared with 6.05 ppm arising from σ electrons. In addition, the figures show a significant sigma-pi mixing induced by the external field in the region of carbons. The π circulation is prevalently paramagnetic around the carbon atom, which explains the negative value characterizing the π contribution to σ_{yy} of its nucleus, ~ -15 ppm.[1]

It must be noted that the theoretical σ_{yy} of proton, ~ 18 ppm, is quite comparable in magnitude with σ_{zz} (~ 16 ppm), whereas σ_{xx} (~ 27 ppm).[1] Since, obviously, such a low value of σ_{yy} must be attributed to the partial deshielding due to the magnetic anisotropy of the neighbor carbon, as the drawings clearly show, the low field shift of benzenic protons can be imputed only in part to the delocalized π stream affecting σ_{zz} and an even more important role should be imputed to localized σ circulations.

Figures 11–13 sketch the situation in the plane passing through the carbon atom, parallel to the yz plane. Figure 11 contains a sink-source couple, which makes the analysis of the outer plotted area more difficult. However, the actual behavior could probably be similar to that found in Fig. 13. In addition, it is interesting to observe that σ electrons sustain a diamagnetic current in the close environment of the C nucleus, characterized by high intensity, whereas a weaker paramagnetic flow is exhibited at larger distances. This pattern would explain the small positive contribution of σ electrons to the xx component of carbon shielding tensor $\simeq +14$ ppm.[1] On the other hand, inspection of Figs. 12 and 13 reveals that a deshielding π paramagnetic current takes place around the carbon atom, which possesses an intensity high enough to overcome the diamagnetic σ circulation close to nucleus. This result is also expected from the theoretical results for the total σ_{xx} component of carbon[1] (~ -56 ppm) and confirms the idea of a large $\sigma-\pi$ mixing induced by a magnetic field perpendicular to the plane of the plot.

Eventually, we have computed the theoretical σ_{zz} along a circumference of radius $r_{CC}+r_{CH}$, whose center is coincident with that of benzene (see Fig. 15) where σ,π contributions and total values are specified as a function of the azimuthal angle α. It is interesting to observe that the proton, lying on the x direction at $\alpha=0°$, is the locus of maximum (minimum) shielding due to $\sigma(\pi)$ electrons, whereas a minimum (maximum) is found at $\alpha=30°$, at the intersection of the circumference and the binary axis bisecting a C–C bond. If the π electrons flowed freely according to the RCM, e.g., with the same intensity all over any point of a same loop, the π contribution to $\sigma_{zz}(\alpha)$ would be a straight line. In any event, because of the reinforcement of the π current near a carbon atom [see Figs. 6(b) and 6(c)], one expects the actual curve not to be flat and the protons to be more deshielded than the other points of the circumference. On the other hand, the oscillation between maximum and minimum amounts to only 0.4 ppm. This is a small

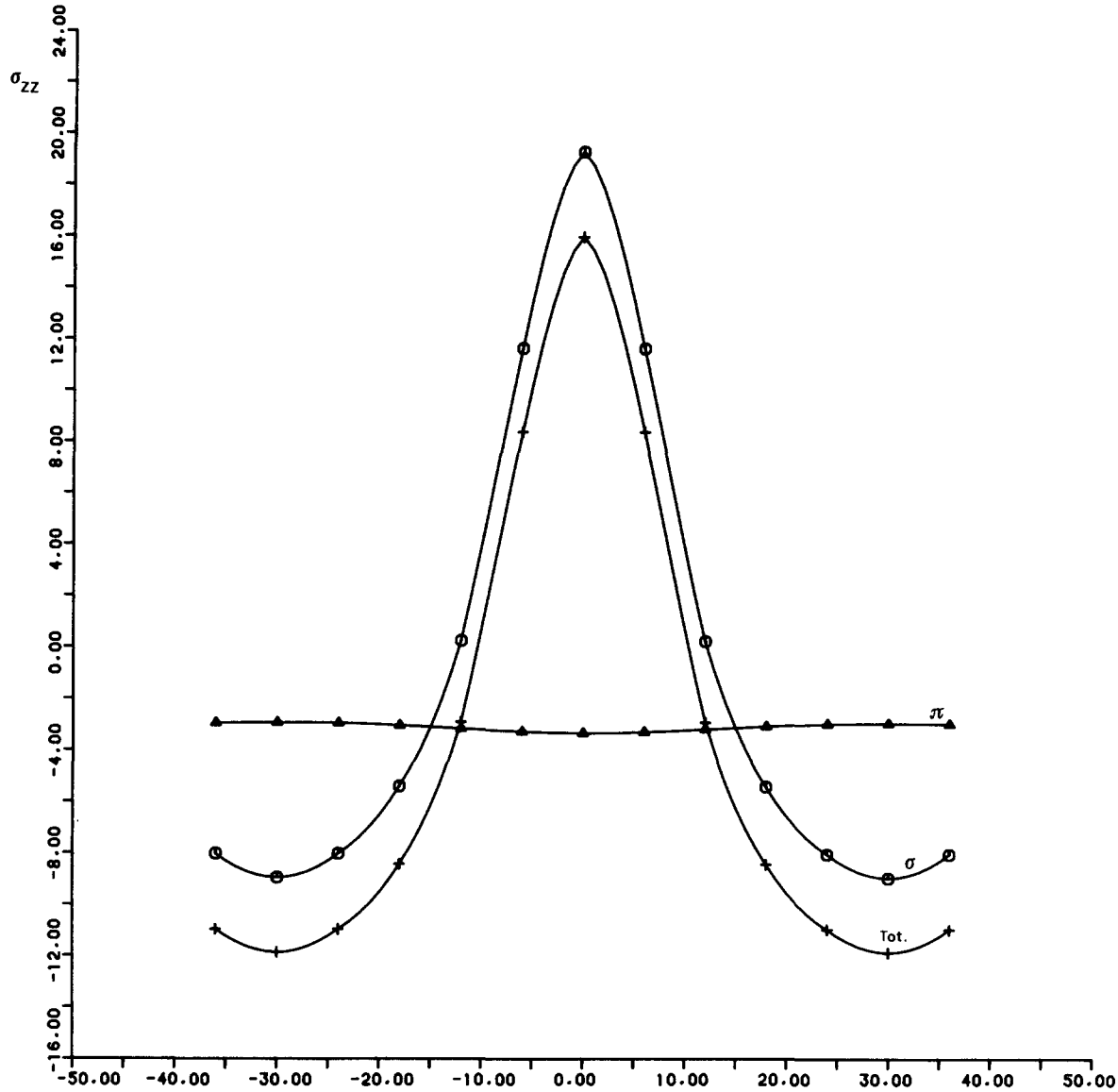

FIG. 15. The σ_{zz} component of magnetic shielding as a function of the d azimuthal angle along the circumference centered on the origin of coordinates and passing on hydrogens. The oscillation of the π contribution, with minimum on protons, is 0.40 ppm.

difference indeed, which, however, does not per se imply the validity of RCM. As a matter of fact, the quasi-flat behavior could also be interpreted within the framework of Musher's picture,[27] in terms of localized effect due to adjacent carbons, which concur to determine $\sigma_{zz}(\alpha)$ along the different points of the circumference. The behavior of the contribution provided by σ electrons is easily understood by inspection of Fig. 1; in particular, the minimum in the curve corresponds to a highly deshielded point near to the paramagnetic AV facing the inlet H–C–C–H. In addition, because of the trend of π contributions, the total σ_{zz} is represented by a curve quite similar to that relative to σ electrons, shifted by $\simeq -3$ ppm.

IV. CONCLUSIONS

According to our findings, the RCM seems to provide a rather oversimplified approach to the understanding of the chemical shift of benzenic protons. Even if our calculations lend some support to the idea of π interatomic currents as an important cause of deshielding for protons, other significant factors clearly emerge which evidence some *ad hoc* character of RCM and the need for an improved model:

(i) For carbon, the nuclear shielding constants seem to be essentially determined by the local regime of streamlines.

(ii) On quantitative grounds, effects arising about a neighboring carbon atom or C–C bonds, where intense diamagnetic electron circulation is induced by the external field, seem to be even more responsible of proton deshielding than delocalized currents.

(iii) The diamagnetic stream does not exhibit any "superconducting" character (which is an unphysical hypothesis[27] and, even if delocalized all over the ring,

is significantly reinforced in the environment of a carbon atom, whereas the RCM assumes a mobile π cloud flowing with equal intensity in every point of a loop. This could imply that, also, π electrons lower σ_{zz} of protons mainly through a local mechanism.

(iv) As evident by symmetry considerations,[27] also σ electrons are capable of sustaining delocalized currents which are diamagnetic in the tail regions and paramagnetic about the center of the molecule. The AV appearing in the center of the molecule is characteristic of planar aromatic molecules and its existence can be predicted merely through topological considerations [1b].

(v) The phrase ring current, which has been retained within the RCM, possesses no more than a historical value, related to the acceptation of London. In fact, every current σ or π induced by a magnetic field is a ring current flowing in a closed loop because of symmetry and continuity requirements. This is nowadays well accepted in the literature, where the expression ring current has been properly used also for BH.[15]

ACKNOWLEDGMENTS

The authors wish to thank Professor R. Moccia and Professor G. P. Arrighini of Pisa University for helpful discussions and suggestions, and Dr. I. Grossi of the staff operating at the Computing Center of North Eastern Italy, Casalecchio di Reno, Bologna, for technical assistance. Thanks are also due to the Computing Center of Modena University for generous allocation of computer time. This work was also supported, in part, by the Italian CNR.

[1]P. Lazzeretti and R. Zanasi, J. Chem. Phys. **75**, 5019 (1981). This paper contains an extended bibliography on the questions concerning the validity of the ring current model, P. Lazzeretti, E. Rossi, and R. Zanasi, Nuovo Cimento D **1**, 70 (1982).
[2]J. A. Pople, J. Chem. Phys. **41**, 2559 (1964).
[3]M. Barfield, D. M. Grant, and D. Ikenberry, J. Am. Chem. Soc. **97**, 6956 (1975).
[4]J. A. Pople, W. G. Schneider, and H. J. Bernstein, *High-Resolution Nuclear Magnetic Resonance* (McGraw-Hill, New York, 1959), p. 180.
[5]P. Lazzeretti and R. Zanasi, Chem. Phys. Lett. **80**, 533 (1981).
[6]L. Landau and E. Lifshitz, Mécanique Quantique, MIR, Moscow, 1966), p. 509.
[7]E. Madelung, Z. Phys. **40**, 322 (1926).
[8]L. Landau, J. Phys. USSR **5**, 71 (1941).
[9]F. London, Rev. Mod. Phys. **17**, 310 (1945).
[10]J. O. Hirschfelder, A. C. Cristoph, and W. E. Palke, J. Chem. Phys. **61**, 5435 (1974).
[11]J. O. Hirschfelder, C. J. Goebel, and L. W. Bruch, J. Chem. Phys. **61**, 5456 (1974).
[12]J. O. Hirschfelder and K. T. Tang, J. Chem. Phys. **64**, 760 (1976); **65**, 470 (1976).
[13]D. F. Heller and J. O. Hirschfelder, J. Chem. Phys. **66**, 1929 (1977).
[14]J. O. Hirschfelder, J. Chem. Phys. **67**, 5477 (1977).
[15]C. T. Corcoran and J. O. Hirschfelder, J. Chem. Phys. **72**, 1524 (1980).
[16]J. Riess, Ann. Phys. **57**, 301 (1970); **67**, 347 (1971); Phys. Rev. D **2**, 647 (1970); Phys. Rev. B **13**, 3862 (1976).
[17]J. Riess and H. Primas, Chem. Phys. Lett. **1**, 545 (1968).
[18]E. A. McCullough, Jr. and R. E. Wyatt, J. Chem. Phys. **54**, 3578 (1971).
[19]R. M. Stevens, R. M. Pitzer, and W. N. Lipscomb, J. Chem. Phys. **38**, 550 (1963).
[20]R. M. Stevens and W. N. Lipscomb, J. Chem. Phys. **40**, 2238 (1964); **41**, 3710 (1964).
[21]R. A. Hegstrom and W. N. Lipscomb, J. Chem. Phys. **45**, 2378 (1966); Rev. Mod. Phys. **40**, 354 (1968).
[22]E. A. Laws, R. M. Stevens, and W. N. Lipscomb, J. Chem. Phys. **54**, 4269 (1971).
[23]W. N. Lipscomb, in *Theoretical Chemistry*, edited by W. Byers-Brown (Butterworths, London, 1972).
[24]S. T. Epstein, J. Chem. Phys. **42**, 2897 (1965); **58**, 1592 (1973).
[25]See, for instance, W. Pauli, Rev. Mod. Phys. **13**, 203 (1941).
[26]G. P. Arrighini, M. Maestro, and R. Moccia, J. Chem. Phys. **49**, 882 (1968).
[27]J. I. Musher, J. Chem. Phys. **43**, 4081 (1965).
[28]F. London, J. Phys. Radium **8**, 399 (1937).
[29]This test was suggested by R. Moccia (private communication).